Intracavity Rayleigh/Mie scattering for multi-point two-component velocity measurement

Daniel Bivolaru, Paul M. Danehy and Joseph W. Lee

NASA Langley Research Center, Advanced Sensing and Optical Measurement Branch, 18 Langley Blvd., Hampton VA 23681, USA

Abstract: A simultaneous multi-point two-component Doppler velocimeter is described. The system uses two optical cavities: a Fabry-Perot etalon and an optical cavity for collecting and re-circulating the Rayleigh/Mie scattered light that is collected from the measurement volume in two parallel, but opposite directions. Single-pulse measurements of two orthogonal components of the velocity vector in a supersonic free jet were performed to demonstrate the technique. The re-circulation of the light rejected by the interferometer input mirror also increased the signal intensity by a factor of 3.5. © 2005 Optical Society of America

Interferometric Rayleigh scattering has previously been used for single-point velocity measurements in unseeded gas flow. However, this past work has generally been limited to probing with continuous-wave lasers resulting in time-averaged measurements of velocity. Multiple velocity components have been measured simultaneously by separate instruments.[1,2] It has also been demonstrated that two orthogonal velocity components can be measured simultaneously at one point using one interferometer by reflecting back the probing laser beam, although this approach results in directional ambiguity of the flow velocity vector.[3] This measurement ambiguity was removed by prior knowledge of the approximate magnitude and sign of the velocity components. Furthermore, it was shown that multiple points could be measured simultaneously with a Rayleigh scattering interferometric approach, but only one component of velocity was measured.[4] Another method of performing multiple component velocity measurements with Rayleigh scattering uses a pair of cameras to image the flow, one of which views the flow through an iodine gas filter. This iodine-filter technique has the advantage of allowing high-resolution velocity imaging, but it generally has a lower dynamic range.[5,6,7]

In this paper, we introduce an improved diagnostic system for time-resolved multi-point measurement of two components of velocity in gas flow using one interferometer. The system extends the interferometric Rayleigh scattering velocimetry techniques described above by employing an additional optical cavity for collecting Rayleigh/Mie scattered light from the measurement volume in two parallel, but opposite directions. The cavity can be used to re-circulate the light rejected by the interferometer, thus considerably increasing the number of photons detected. In this case, a measurement ambiguity exists. To remove the measurement ambiguity, an estimate of the sign and magnitude of the velocity components is required to be known before the measurement. Alternately, the second optical cavity can be detuned to totally remove the measurement ambiguity. However, in this case re-circulation is no longer possible.

The scattering geometry is illustrated in Fig. 1, which also shows the optical setup of the instrument. The Doppler shift frequency of the scattered light collected in the direction of $\mathbf{k}_{s1}$ is given by $\Delta\nu_1 = (\mathbf{k}_{s1} - \mathbf{k}_0) \cdot \mathbf{V}$, where the $\mathbf{k}_{s1}$ and $\mathbf{k}_0$ are the wave vectors of the scattered and incident light respectively. The direction of $(\mathbf{k}_{s1} - \mathbf{k}_0)$ vector gives the direction of the velocity component that is measured. If a second collection optic is placed along the same optical axis, but on the opposite side of the probed region, the scattering wave vector is $\mathbf{k}_{s2} = -\mathbf{k}_{s1}$, where $|\mathbf{k}_{s1}| = |\mathbf{k}_{s2}| = |\mathbf{k}_0|$. A mirror is used to reflect this collected light along the optical axis, sending it back to the interferometer. This light shows a Doppler shift $\Delta\nu_2 = (\mathbf{k}_{s2} - \mathbf{k}_0) \cdot \mathbf{V}$ and the velocity component is measured along the vector $(\mathbf{k}_{s1} + \mathbf{k}_0)$, i.e. the two measured components are orthogonal.

The Rayleigh scattered light in the $\mathbf{k}_{s1}$ direction is collected and collimated by the L_2 lens. The beam diameter is reduced to match the interferometer's input-aperture diameter using a beam reducer/expander, lenses L_3 and L_4. The light is mixed together with laser light before it is passed through the Fabry-Perot interferometer (F-P) using the beam combiner (BC). Referencing the Rayleigh/Mie scattered light with unshifted laser light in a single interferogram reduced the velocity measurement uncertainty by decreasing the adverse effects of the laser frequency drift, interferometer alignment errors, vibrations, and background light scattering.[8] A small fraction of this mixed light is transmitted through the interferometer, but most of it (~98%) is reflected back toward the measurement volume. In the usual arrangement (not containing Mirror M_r and lens L_1) this rejected light is lost. In the optical arrangement shown in Fig. 1, the reflected light is focused by the lens L_2, collected and collimated by lens L_1 and reflected back on the optical axis by the mirror M_r. Similarly, in the $\mathbf{k}_{s2}$ direction, the light is collected and collimated by the lens L_1 and reflected toward the interferometer by the mirror M_r. This cycle continues until all

energy of the collected light is transmitted through the interferometer or lost. Losses are due to absorption, scattering, and consecutive reflections in the optical components.

At the output of the interferometer, a high-sensitivity CCD camera images the interference fringe pattern. The optics are arranged so that the probed region is imaged through the etalon [4]. Therefore the interferogram contains spatial as well as spectral information. Each set of fringes along the laser's path in the image corresponds to different measurement locations in the flow. A limitation of this method is that the field of view is restricted to a small region at the focusing point of lens L_1 because the light is required be collimated and perpendicular to the etalon input mirror. Image processing software is used to analyze the interferogram for the Doppler shift of the Rayleigh/Mie signal and the laser frequency, and to solve for velocity.[8] An interferogram containing both the Rayleigh scattered signal (a straight horizontal line pattern) and the reference laser frequency information (concentric rings) is shown in Fig. 2a and 2c.

In the experiments reported here we used a pulsed Nd:YAG laser at 10 Hz and 9 nsec/pulse, with 65 mJ/pulse. Experiments were performed in stagnant air and a 1.5-mm diameter under-expanded supersonic jet flow. The jet exhausts into ambient air and has a stagnation chamber temperature of 296 K or lower and a stagnation pressure of 5.2 atm. A low velocity co-flow of air was used to minimize contamination by dust particles. We probed a volume about 1.5 mm length and 0.2 mm diameter located at 10 nozzle diameters from the nozzle exit. The separation distance between the first two consecutive fringe orders on one side of the interferogram corresponds to about 0.2 mm in the flow.

When Mie scattering (from water clusters, for example) is predominant, the scattered light intensity is orders of magnitude larger than the Rayleigh scattering intensity. In this case, the light re-circulation is not necessary, but can be very useful for combining the signal on the same optical axis, allowing for minimal optics, simplified alignment, and high efficiency. However, if the mirror M_r is oriented perpendicular to the optical axis, the spectra of scattered light from both collection directions overlap on the interferogram. Then, the peaks corresponding to different velocity components cannot be separated. This ambiguity can be overcome if the experiment is designed so that one measured velocity component is always much bigger than the other (Fig. 2b). For example, the axial velocity component in a high-speed jet is generally much larger than the radial component. An alternative way to remove this ambiguity is to slightly detune the external cavity in the vertical direction. The new image will contain two parallel

lines situated symmetrically around the center of the interferogram, as shown in Fig. 2c, each horizontal line representing one measurement direction.

To compute the flow velocity, five rows were averaged through the center of the interferogram shown in Fig. 2b. This data was converted from the spatial domain (pixels) to the frequency domain as described in reference [8]. Two spectra processed in this way are shown in Fig. 3. Gaussian functions were fitted to this data to determine with sub-pixel resolution the location of the peaks and implicitly the frequency. The low frequency peak slightly above 3 GHz in the spectrum is the reference frequency (laser frequency) used to identify the zero-velocity fringe location. The first peak in each spectrum is the Doppler shifted peak associated with the V_1 component and the middle peak with the V_2 component. The two sets of peaks shown in Fig. 3 (corresponding to the left and right sides of the interferogram in Fig. 2b) show the simultaneous measurement at two locations in the flow situated at about 0.5 mm apart. The calculated Doppler shifts of the peaks are 0.98 GHz (left) and 1.38 GHz (right) for the V_1 component, and 0.53 GHz (left) and 0.60 GHz (right) for the V_2 component. These frequency shifts correspond to velocity measurements of 370, 520, 200, and 230 m/s respectively. The error in determining these frequencies is influenced by the measurement of the free spectral range of the interferometer but is dominated by the errors during data extraction from the interferogram and during fitting. A careful selection of the optical setup to have an increased resolution of the interferogram and an increased number of photons per pixel received will minimize these errors. Further errors are incurred when converting these Doppler shifts to velocity because of uncertainties in the measurement of the angles between the probing laser and the light collection optics.

The significantly different Doppler shifts at these two locations prove the system's capability for simultaneous multipoint measurements. In principle, the next outer fringe patterns (not shown in Fig. 3) can also be analyzed for velocity, but with reduced resolution.

To analyze the photon collection efficiency of the system, Rayleigh scattered light was collected in room air. To obtain a more accurate evaluation of the total number of photons accumulated by the detector, the reference light was purposely not injected into the system. An area of 100 x 100 pixels of the interferogram was used for this investigation. The Rayleigh spectrum for measurement of one component of velocity and the spectrum for simultaneous measurement of two components of velocity using the light re-circulating cavity (high amplitude curve) are compared in Fig. 4.

Considering that both collecting optics received approximately the same number of photons, re-circulating the light rejected by the interferometer input mirror increased the total number of photons reaching the detector by nearly 3.5 times. Conversely, the maximum intensity per pixel detected for each velocity component increased by 81%. Any slight misalignment or optical aberrations also contributes to the spreading of the beam over a larger area, reducing the maximum number of photons detected per pixel and also reducing the spatial resolution of the measurement.

In conclusion, the use of a secondary cavity enabled the simultaneous multi-point measurement of two orthogonal components of velocity using a single interferometer. Additionally, the cavity recycled the light rejected by the interferometer's input mirror, greatly increased the number of photons reaching the detector and improved the signal-to-noise ratio. Two methods of using this second cavity to measure gas velocity were demonstrated: one yielding higher signals and the other allowing unambiguous velocity measurement.

We wish to express our appreciation to Mr. George Rumford, program manager of the Defense Test Resource Management Center's (DTRMC) Test and Evaluation/Science and Technology (T&E/S&T) program, for funding this effort under the Hypersonic Test focus area. Also, we wish to thank Jim Meyers at NASA Langley Research Center for invaluable discussions and for the use of his laboratory and equipment.

References

[1] Seasholtz, R.G., Goldman, L. J., "*Three Component Velocity Measurements Using Fabry-Perot Interferometer*", Second International Symposium on Applications of Laser Anemometry to Fluid Mechanics sponsored by 'Instituto Superior Tecnico (Lisbon)', Lisbon, Portugal, July 2-4, 1984 (also NASA TM 83692)

[2] Seasholtz, R.G., Goldman, L. J., "*Combined Fringe and Fabry-Perot Laser Anemometer for Three Component Velocity Measurements in Turbine Cascade Facility*", AGARD Conference Proceedings No.399, Advanced Instrumentation for Aero Engine Components, Presented at the Propulsion and Energetics Panel 67th Symposium, Philadelphia, PA, USA, pp. 13-1 to 13-15, 19-23 May 1986.

[3] Eggins, P. L., and Jackson, D. A.,"*A two-component laser-Doppler anemometer using a single Fabry-Perot interferometer*," J. Phys. **D:** Appl. Phys., Vol. 8, pp. 45-47, 1975.

[4] Seasholtz, R.G., Instantaneous 2D Velocity and Temperature Measurements in High Speed Flows Based on Spectrally Resolved Molecular Rayleigh Scattering", *AIAA 33rd Aerospace Sciences Meeting*, Reno, AIAA-95-0300, January 9-12, 1995.

[5] Elliott, G.S., Glumac, N. and Carter, C.D. "*Molecular Filtered Rayleigh Scattering Applied to Combustion,*" Measurement Science and Technology, Vol. 12, No. 4, pp. 452-466, 2001.

[6] Miles, R., B., Lempert, W., and Forkey, J., N., "*Laser Rayleigh Scattering,*" Reviw Article, Measurement Science and Technology, Vol. 12, No., pp. 33-51, 2001.

[7] Meyers J.F. '*Development of Doppler global velocimetry as a flow diagnostics tool,*' Meas. Sci. Technol. 6, pp.769-783. 1995.

[8] Bivolaru, D., Ötügen, M. V., Tzes, A. and Papadopoulos, G., "*Image Processing for Interferometric Mie and Rayleigh Scattering Velocity Measurements*", AIAA Journal, Vol. 37, No. 6, pp. 688-694, 1999.

Figure Caption:

Fig. 1 Optical setup for measurement of two orthogonal components of flow velocity.

Fig. 2. Fabry-Perot interferograms. (a) Rayleigh scattering in static room air, (b) Mie scattering in a supersonic jet with mirror M_r exactly aligned onto the optical axis – close-up view of the first two fringe patterns, and (c) Rayleigh scattering in the supersonic jet with mirror M_r angled slightly to separate the two collection directions.

Fig. 3. Spectra of Mie and Rayleigh scattering from water clusters generated naturally in the flow. The distance between the left and right measurement points was about 0.5 mm in the flow.

Fig. 4 Rayleigh spectrum in stagnant air without reference laser frequency.

Figures:

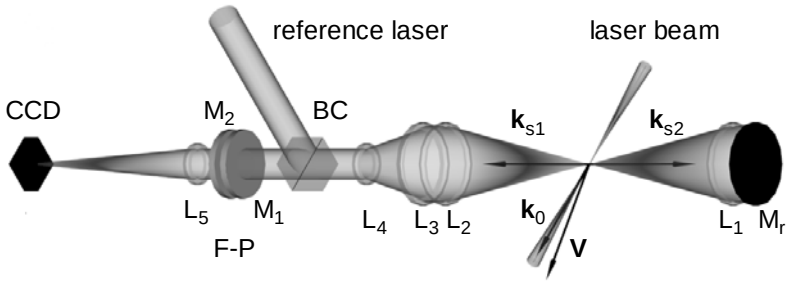

Fig. 1 Optical setup for measurement of two orthogonal components of flow velocity.

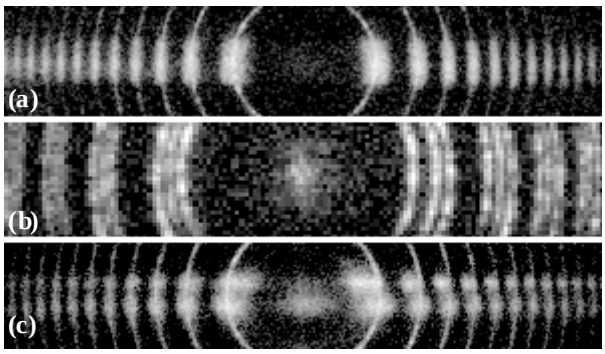

Fig. 2. Fabry-Perot interferograms. (a) Rayleigh scattering in static room air, (b) Mie scattering in a supersonic jet with mirror M_r exactly aligned onto the optical axis – close-up view of the first two fringe patterns, and (c) Rayleigh scattering in the supersonic jet with mirror M_r angled slightly to separate the two collection directions.

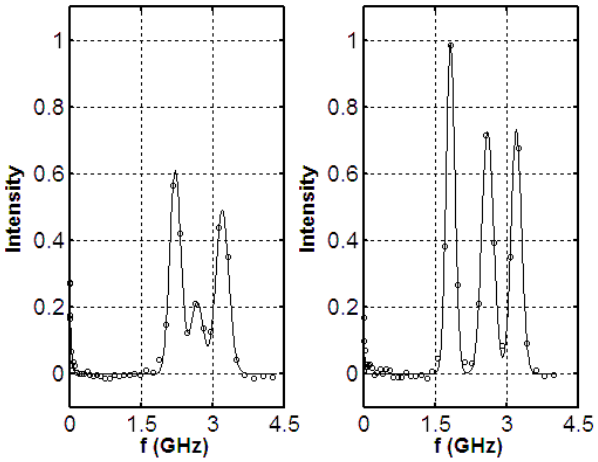

Fig. 3. Spectra of Mie and Rayleigh scattering from water clusters generated naturally in the flow. The distance between the left and right measurement points was about 0.5 mm in the flow.

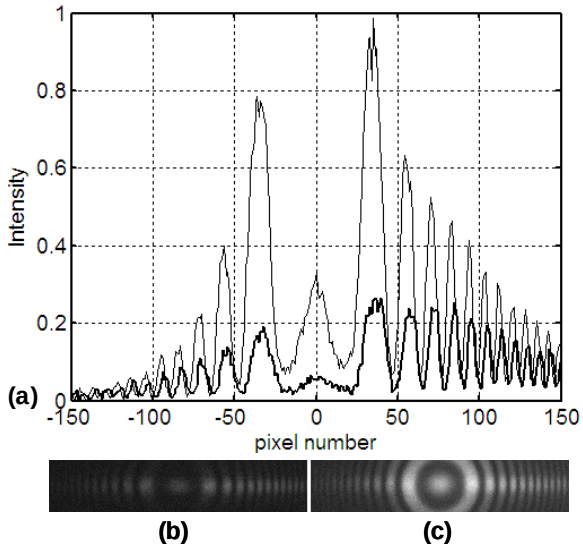

Fig. 4 Rayleigh spectrum in stagnant air without reference laser frequency.